Research Journal of Applied Sciences, Engineering and Technology 2(4): 319-325, 2010
ISSN: 2040-7467

Submitted Date: March 12, 2010 Accepted Date: May 08, 2010 Published Date: July 10, 2010

Fatigue Crack Initiation Analysis in 1060 Steel

[1]L. Gyansah and [2]A.K. Ansah
[1]Department of Mechanical Engineering
[2]Department of Computer Science and Engineering,
University of Mines and Technology, Tarkwa, Ghana

Abstract: This study investigates initiation of small cracks on dumble-shaped plate type specimens of 1060 steel at the load ratio of R = 0 under varied cyclic stress amplitudes between 0.6 and 1.0 of yield stress using the Instron machine (model: 8501). Sinusoidal wave of a frequency of 10 Hz was used in the experiment. The experiment was conducted at a room temperature of 23ºC. Each test for different applied stress ranges was carried out for 2×10^4 cycles. Microstructure and fractography of the fractured specimen were also analyzed. Nucleations of cracks were observed at Ferrite-Ferrite Grain Boundary (FFGB) as well as inside Ferrite Grain Body (FGB), but the FFGB location was preferred. Results show that the average length of FFGB cracks is found larger than that of the average length of cracks initiated inside FGB at the same cyclic loading conditions. The formation of slip band inside grain body, slip band impingement at grain boundary and elastic-plastic incompatibility synergistically have significant influence on fatigue crack initiation in 1060 steel. Additionally, the formation of irregular voids inside slip bands, initiation and growth of small voids at grain boundary and the subsequent joining of these with other voids were seen as specific characteristics of 1060 steel. It was also established that cracks nucleate both at grain boundary and inside grain body in 1060 steel in the investigated domain of 0.6 to $1.0\sigma_y$. It was further established that the orientation of the grain body cracks at low stress level is greater than 45º and the average angle of orientation of these cracks increases like that of grain boundary cracks with increased magnitude of stress range.

Key words: Crack initiation, cyclic loading, fatigue, ferrite grain body, ferrite grain boundary, fractography, growth, small crack, 1060 steel

INTRODUCTION

The development of 1060 steel has been a milestone for achieving high drawability of sheet steels and is being increasingly considered as material for the automotive industry in Ghana. 1060 steel is necessarily medium carbon variety from which has a carbon content of 0.60 wt% (Bolton, 2000). The initial emphasis on the development of this steel has been laid on its manufacturing route and in seeking correlation between structure (related to grain size, texture and anisotropy ratio etc.,) and properties (related to strength, formability and drawability etc.,) for varied material chemistry and thermo-mechanical treatment) (Dowling, 1993). Since this steel is primarily developed for automotive application, its cyclic damage behavior and fatigue properties are of paramount interest, but unfortunately investigations in this direction are limited. The fatigue damage in a structural component consists of several sequential stages like: (a) sub-structural changes causing nucleation of micro-cracks, (b) formation of micro-cracks, (c) growth and coalescence of micro-cracks to a dominant macro-crack, Kwofie, (2000) (d) stable propagation of the dominant macro-crack, and finally (e) structural instability causing complete fracture (Spotts, 1971). The design philosophy against fatigue damage either considers all the stages or it considers only the stable sub-critical propagation of the dominant macro-crack (Barsom and Rolfe, 1987). It is well conceived by now that a large percentage of fatigue life of smooth specimens are spent in the domain of crack nucleation and small or short crack growth, especially in the emerging clean structural materials in high cycle fatigue (Cottrell, 1979). It is thus imperative to gather more knowledge about crack nucleation and about small or short crack growth behavior in 1060 steel. The instant of crack initiation is difficult to separate from the stage of small or short crack propagation in a material (Shank, 1953). Any crack with all three dimensions small is defined here as 'small crack' (Bray and Roderic, 1997). The 'short cracks' are in addition known to possess two small dimensions and the third one mimic that of macroscopic size. Fascinatingly, the developments related to the mechanisms of crack nucleation are found to be mostly associated with concepts related to sub-structural features like dislocations, dislocation-vacancy complexes, dislocation dipoles etc. whereas the models describing small/short crack growth behavior in materials emphasizes on accounting the microstructural features

Corresponding Author: L. Gyansah, Department of Mechanical Engineering, University of Mines and Technology, Tarkwa, Ghana

Table 1: Composition of 1060 steel

Weight (%)	Carbon (C)	Manganese (Mn)	Phosphorus (P)	Sulfur(S)	Iron (Fe)
	0.61	0.56	0.03	0.05	98.75

like grain boundaries, precipitates and second phase particles (Askeland, 1989). Principally in 1060 steel, the phenomenon of crack initiation and small crack growth are of great scientific interest because the cyclic damage of the predominantly body-centered cubic (bcc) ferritic structure would be governed by the typical behavior of screw dislocations having extended core inducing slip asymmetry in cyclic deformation during the initiation stage whereas its growth would probably be controlled by the grain size and the sub-microscopic precipitate particles (Childs, 2000). The major aims of this paper are to identify the preferred crack nucleation sites in 1060 steel and to distinguish the possible mechanisms associated with the various types of cracks observed in the material.

MATERIALS AND METHODS

The 1060 steel was obtained from the University of Mines and Technology, Ghana. The experiment was conducted in the University of Mines and Technology, Mechanical Engineering Laboratory in December 2009. The composition of the 1060 steel is shown in Table 1. 1060 steel comprises of Carbon, Manganese, Phosphorus, Sulfur and Iron. Their weight percentages are illustrated in Table 1.

Sample preparation: Specimen was obtained as hot rolled plates, machined and grinded. The test specimen was polished to be free of nicks, dents, scratches, and circumferential tool marks. This was done to reduce the degree of crack initiations. Compressed air was blown on the surface of the specimen to remove dirt particles.

Sample design: The nature of the specimen is illustrated in Fig. 1. Specimen was cut into the requisite shape by the use of the power hacksaw and the lathe machine. The alphabet *R* is the radius of the arc. All measurements are in millimetre (mm).

Experimental: Microstructural test, tensile test, fatigue test and fractographical test were done on the specimen.

Microstructural test: Specimens for microstructural analysis were ground with emery paper and were polished using alundum and finally using 0.25 μm diamond paste. The polished specimens were then etched with 2% Nital solution to expose the microstructure. Microscopic examination indicates the 1060 steel contain both ferrite and pearlite. This is illustrated in Fig. 2. The average grain size was found to be 64.3±1.3 μm by linear intercept method.

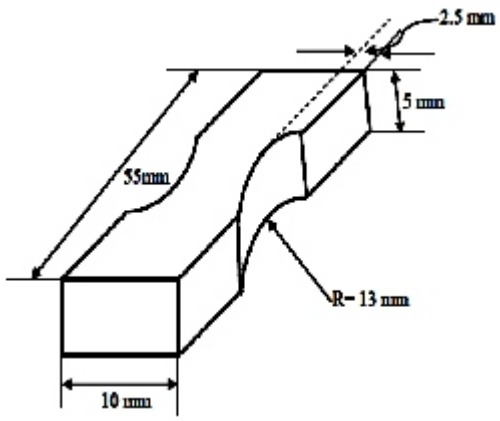

Fig. 1: Sample design of 1060 steel

Tensile test: Cylindrical specimens of 5 mm gauge diameter and 22 mm gauge length were used in the tensile test of the 1060 steel (ASTM, 2003). The tests were performed using the Universal tensile testing machine (Schimadzu, model: AG-5000G) at a nominal strain rate of 4.1×10^{-4}/s at a room temperature of 23ºC. From the test, the average yield strength and tensile strength of the specimen was found to be 95±2 and 243±3 MPa, respectively.

Fatigue and fractographic test: Fatigue tests were done on the specimen configuration shown in Fig. 1. One surface of the specimens was ground, polished and etched to expose the microstructure. The fatigue experiment was performed with the used of the Instron machine (model: 8501) using sinusoidal wave at a frequency of 10 Hz at a room temperature of 23 ºC. The tests are conducted on the various stress ranges keeping the maximum stress as 0.6 to 1.0 (i.e., is yield strength) of the steel while maintaining the minimum stress at zero. Each test for different applied stress ranges was carried out for 2×10^4 cycles. After the fatigue test, the specimens were examined under a scanning electron microscope (SEM) to locate the crack initiation sites Fellows, (1985). Apparently, a series of photographs with cautious demarcation of the loading direction of the specimens were taken from several locations of interest, which actually exhibits small cracks. Substantially, the average length and the orientation of small cracks and their location in the microstructure were again examined.

RESULTS AND DISCUSSION

The location at which cracks initiate in the microstructure of 1060 steel and the nature of such cracks

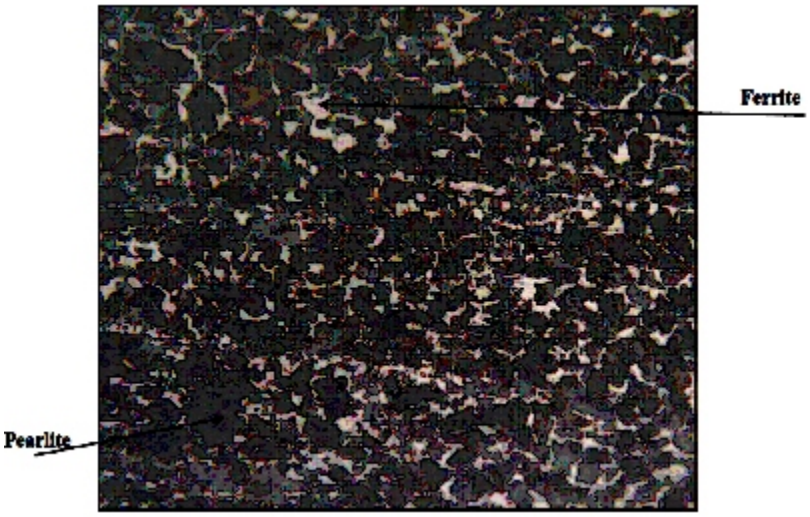

Fig. 2: Typical microstructure of 1060 Steel (300X)

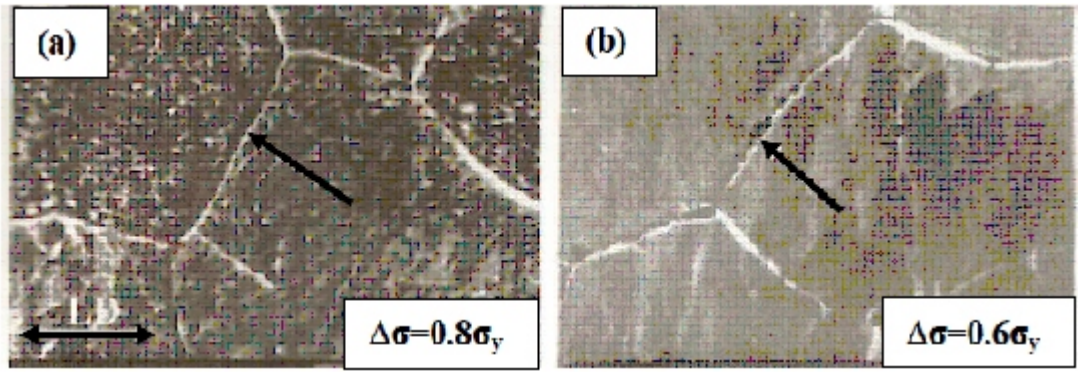

Fig. 3: Ferrite grain boundary cracks in 1060 steel

after a stage of growth to a size where these can be conveniently examined by scanning electron microscopy, are the primary content of this study. The cracks thus examined may be simply termed as "small cracks". In order to understand the influence of the microstructure on the nature of the initiated cracks, the fatigue tests have been carried out in a manner that most of the cracks are generated with negligible growth. The size range of the observed cracks was found to be 2-43, 7-96 and 7-60 μm at a stress range ($\Delta\sigma$) = 0.6, 0.8 and 1.0$_y$ respectively. The cracks exhibit a wide size range under identical ($\Delta\sigma$) and number of cycles (N); because, when one type of cracks gets generated with the lower bound values of the size range, a number of alternate cracks are found to nucleate and grow to sizes near the upper bound. A series of these cracks were photographed using a Scanning Electron Microscope (SEM) at suitable magnifications so that their maximum dimension can be measured conveniently. The SEM examinations of the polished and etched surfaces of the fatigue tested specimens of the 1060 steel indicated that the location at which crack initiation occurs in the microstructure of this steel is either at the grain boundary or in the grain body. Some typical grain boundary and grain body cracks are illustrated in Fig. 3 and 4 respectively. It is therefore interesting to say that the cracks initiation sites for 1060 steel can be demarcated as (a) grain boundary and (b) grain body cracks based on their position in the microstructure. In Fig. 3, the Loading Direction (LD) is common to both microstructures and is drawn in (a). Microstructure (a) illustrates grain boundary crack oriented at 45ºC to the loading axis whiles microstructure (b) illustrates voids and splits at grain boundary together with slip bands.

In Fig. 4 also shows a set of typical ferrite grain body cracks in 1060 steel. In Fig. 4 the microstructure (a) illustrates a formation of crack along slip band. Microstructure (b) presents formation of irregular voids and cracks along slip bands. Microstructure (c) illustrates coalescence of voids to initiate cracks with low aspect ratio. Microstructure (d) shows cracks with sharp tips.

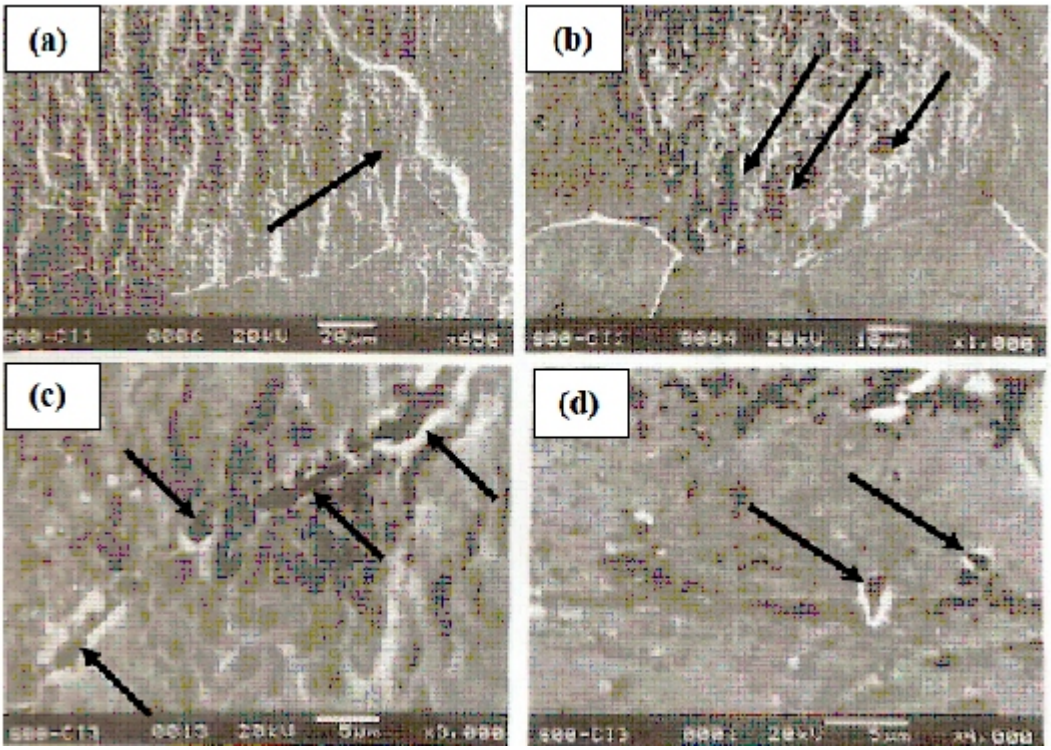

Fig. 4: Ferrite grain body cracks in 1060 steel

Crack initiation analysis in grain boundary: The size and the distribution of grain boundary cracks were analyzed first at different applied fatigue stress ranges ($\Delta\sigma$) and the respective average lengths of these cracks at $\Delta\sigma = 0.6$, 0.8 and $1.0\sigma_y$ were established. These average crack lengths are shown in Table 2.

The result in Table 2 indicates that the average size of the initiated cracks at the lowest stress range of $0.6\sigma_y$ is considerably smaller than that at higher stress ranges. These results thus naturally conclude that some of the initiated cracks at higher stress range ($\Delta\sigma$) got the chance to grow rapidly. Typical distributions of the crack sizes at the imposed stress ranges are illustrated in Fig. 5. Figure 5 to 11 was plotted using Microsoft office Excel (Graver and Barber, 1995). The histogram charts represent the results from the experiment.

From Fig. 5, it is clear that 60% of cracks at $0.6\sigma_y$ possess size less than 10 μm. In addition, 10% of the frequency yielded a crack of 10 to 20 μm.

In Fig. 6, almost 60% of cracks have sizes in the range of 20 to 60 μm. Furthermore, 15% of the frequency yielded cracks in the range of 0 to 20, 40 to 60, and 60 to 80 μm.

In Fig. 7, almost 75% of cracks have sizes in the range of 20 to 60 μm. Furthermore, about 23% of the frequency yielded cracks in the range of 0 to 20 μm whilst 10% of the frequency has crack sizes in the range of 60 to 80 μm.

Orientations of grain boundary cracks: The orientations of the observed grain boundary cracks with respect to loading axis were also analyzed and the data are plotted in Fig. 8-10. Table 3 shows the average angle of orientation for the grain boundary crack with respect to the loading axis for the various applied stress ranges of $0.6\sigma_y$, $0.8\sigma_y$ and $1.0\sigma_y$.

In Fig. 8, it could be seen clearly that the majority of the $0.6\sigma_y$ bear orientation between 30 to 60°. At higher stress ranges as shown in Fig. 9 and 10, larger amount of cracks bear orientation greater than 60º. The average angle of orientation of the grain boundary cracks with respect to the loading axis for is also shown in table 3. These results indicate that crack initiation occurs primarily in the direction of maximum shear planes, which coincide with the available grain boundary orientations in the microstructure. The higher angle of crack orientation at higher stress levels can be attributed either to the possible joining of more than one crack or extension of the cracks through adjacent grain boundaries. In summary it can be inferred that the average size of the initiated cracks (at the lowest stress range of $0.6\sigma_y$) in 1060 steel is 146 mm and their average angle of orientation with respect to the loading axis is approximately 45º.

Crack initiation analysis in grain body: Comparing grain boundary cracks to grain body, it was observed that

Table 2: Average crack length along grain boundary

	Fatigue stress range		
Average crack length	0.6 σ_y (146) μm	0.8 σ_y (387) μm	1.0 σ_y (344) μm

Table 3: Average angle of orientation in grain boundary cracks

	Fatigue stress range		
Average angle of orientation	0.6 σ_y (445)°	0.8 σ_y (497)°	1.0 σ_y (596)°

Table 4: Average crack length in grain body

	Fatigue stress range		
Average crack length	0.6 σ_y (85) μm	0.8 σ_y (153) μm	1.0 σ_y (146) μm

Table 5: Average angle of orientation for grain body

	Fatigue stress range		
Average angle of orientation	0.6 σ_y (6015)°	0.8 σ_y (6312)°	1.0 σ_y (822)°

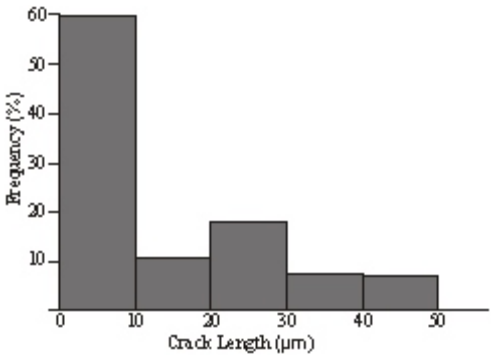

Fig. 5: Distribution of grain boundary crack in 1060 steel at 0.6

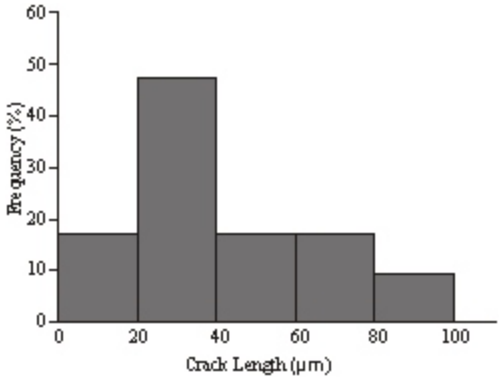

Fig. 6: Distribution of grain boundary crack in 1060 steel at 0.8

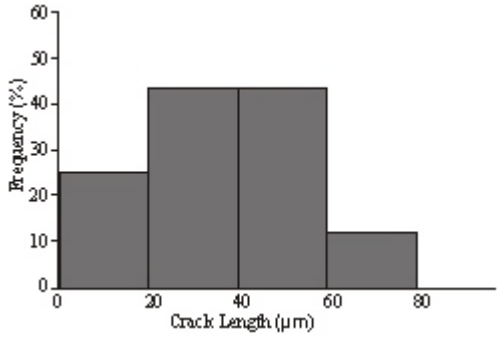

Fig. 7: Distribution of grain boundary crack in 1060 steel at 1.0

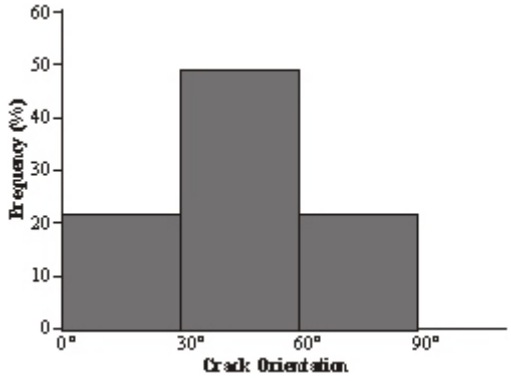

Fig. 8: Distribution of orientation of grain boundary crack in 1060 steel at 0.6

the number of cracks noted at grain boundaries more than that observed in grain body. The average crack lengths at stress range of 0.6 σ_y, 0.8 σ_y and 1.0 σ_y are shown in Table 4.

The average length of cracks in the grain body at lower stress ranges is thus found to be considerably smaller than that found in the grain boundaries. Figure 11 shows a comparison of the crack lengths in grain boundary and at the grain body at different stress levels. In Fig. 11, it is clear that the crack length in the grain body continuously increases with increasing applied stress range while that of the grain boundary reaches a plateau

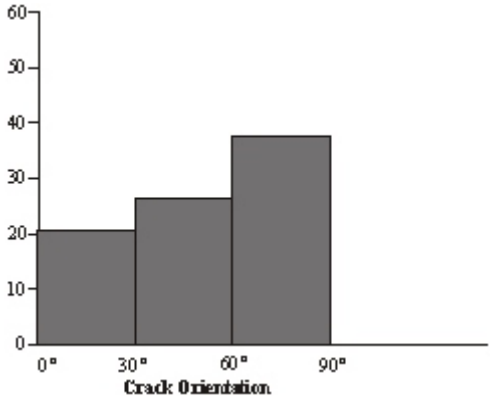

Fig. 9: Distribution of orientation of grain boundary crack in 1060 steel at 0.8

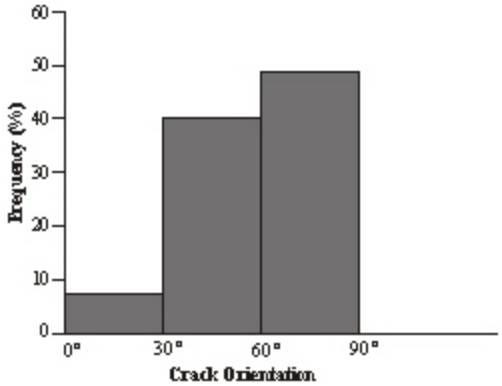

Fig. 10: Distribution of orientation of grain boundary crack in 1060 steel at 1.0

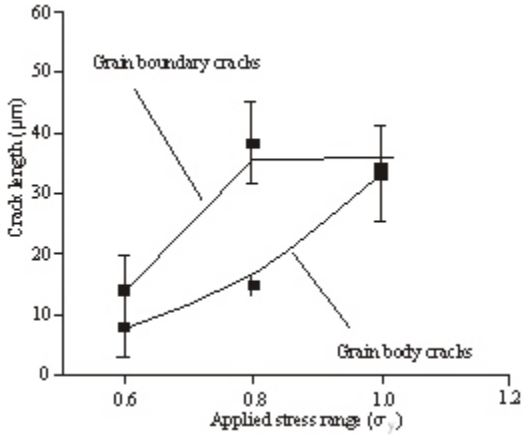

Fig. 11: Average crack lengths versus applied stress range

at that stress range around $0.8\sigma_y$. Fascinatingly, the grain body cracks also meet this plateau at $1.0\ \sigma_y$.

The average orientation of the grain body cracks with respect to the loading axis is illustrated in Table 5. The higher angle of grain body crack orientation concludes that crack initiation in grain body is mainly dominated by normal stresses.

CONCLUSION

Based on the results obtained, the following conclusions can be drawn from the fatigue crack initiation of 1060 steel;

- The average length of cracks initiated at grain boundaries is larger than the average length of cracks initiated inside grain body at the same cyclic loading conditions.
- The length of an initiated crack in grain body is always smaller at lower applied stress ranges.
- The formation of irregular voids inside slip bands, initiation and growth of small voids at grain boundary and the subsequent joining of these with other voids were seen as specific characteristic of ductile material like 1060 steel.
- At lower stress range, orientation of the grain boundaries cracks in 1060 steel is very close to 45º whilst this is greater than 60º for grain body cracks.
- Cracks nucleate both at grain boundary and inside grain body in 1060 steel in the investigated domain of 0.6 to $1.0\sigma_y$.
- Ferrite-ferrite grain boundaries are found to be significantly preferred crack initiation sites in comparison to ferrite grain body.
- The orientation of the grain body cracks at low stress level is greater than 45º and the average angle of orientation of these cracks increases like that of grain boundary cracks with increased magnitude of stress range.
- The formation of slip band inside grain body, slip band impingement at grain boundary and elastic-plastic incompatibility synergistically have significant influence on fatigue crack initiation in 1060 steel.

RECOMMENDATION

Based on the results obtained, this recommendation was drawn;

- A crack seen as a ‘small crack’ should be taken as a crack that with time will grow and cause failure of the entire structure. Such crack must be investigated and require mitigation measures taken to prevent persistent growing of the crack to cause total failure of the entire structure.

ACKNOWLEDGMENT

The authors are thankful to Prof. Adetunde, I. A, the Dean of Engineering, University of Mines and Technology, Tarkwa, Ghana, Dr J. Yendaw and Mr. J.K Annan, lecturers at University of Mines and Technology,

Tarkwa, Ghana for their advice, valuable comments and suggestions.

REFERENCES

Askeland, D.R., 1989. The Science and Engineering of Materials, PWS. 2nd Edn., Kent Publishing Company, Boston, pp: 90-96.

ASTM, 2003. Standard E 8M-03, Standard Test Methods for Tension Testing of Metallic Materials (Metric). Vol: 03.01, ASTM Annual Book of Standards, ASTM, West Conshonhocken, PA.

Barsom, J.M. and S.T. Rolfe, 1987. Fracture and Fatigue Control in Structures, Applications of Fracture Mechanics. 2nd Edn., Prentice-Hall, Inc., A Division of Simon and Schuster, Englewood Cliffs, New Jersey, pp: 1-26, 223-242.

Bolton, W., 2000. Engineering Materials. 3rd Edn., Pocket Book, Newnes, Oxford, pp: 22-43.

Bray, D.E. and K.S. Roderic, 1997. Nondestructive Evaluation, A tool in Design Manufacturing and Service. Elsevier Butterworth Heinemann, New York, pp: 115-116.

Childs, P.R.N., 2000. Mechanical Design. 2nd Edn., Elsevier, Butterworth Heinemann, New York, pp: 27-29.

Cottrell, A., 1979. An Introduction to Metallurgy. 2nd Edn., Edward Arnold Ltd, London, pp: 422-424.

Dowling, N.E., 1993. Mechanical Behavior of Materials: Engineering Methods for Deformation. Fracture and Fatigue, Prentice-Hall International, New Jersey, pp: 622-633.

Fellows, A.J., 1985. Fractography and Atlas of Fractographs, Metals Handbook. 8th Edn., American Society for Metals, Metals Park, Ohio 44073, 9: 48-49.

Graver, R.T. and M. Barber, 1995. Exploring Microsoft Office 97 Professional. Prentice Hall, New Jersey, 1: 1-32.

Kwofie, S., 2000. Cyclic plastic behaviour and low-cycle fatigue in copper. Ph.D. Thesis, University of Witwatersrand, Johannesburg, pp: 26-30.

Shank, M.E., 1953. A critical review of brittle failure in carbon plate steel structures other than ships. Ship structure Committee Report, Serial No. SSC-65, National Academy of Sciences-National Research Council, Washington, DC, Dec., 1.

Spotts, M.F., 1971. Design of Machine Elements. 4th Edn., Prentice- Hall, Inc., Englewood Cliffs, New Jessey, pp: 71-85.